ALMA Memo 343

11 January 2001

Waveguide Quadrature Hybrids for ALMA Receivers

S. Srikanth and A. R. Kerr
National Radio Astronomy Observatory
Charlottesville, VA 22903, USA

Abstract

This memo describes the design of a set of waveguide quadrature hybrids suitable for use in balanced and sideband-separating mixers, balanced amplifiers, and power combiners and dividers. The hybrids are of the branch-line type, which can be machined in a split block configuration on a CNC milling machine. The prototype designs are for the WR-10 band (75–110 GHz), but the dimensions are chosen to allow scaling to any waveguide band up to ~700 GHz. The designs were optimized using a space mapping procedure, with a fast but approximate microwave circuit simulator (MMICAD) and a slower but accurate FDTD EM simulator (QuickWave).

Introduction and Goals

Quadrature hybrids are used in balanced mixers and amplifiers, sideband-separating mixers, and power dividers and combiners. In developing receivers for ALMA, waveguide quadrature hybrids have been proposed for power combining in the first LO system [1], and for a balanced sideband-separating SIS mixer [2]. The latter requires three RF quadrature hybrids, one for sideband separation and one for each of the component balanced mixers.

A quadrature hybrid is a four-port directional coupler. In the ideal case, power incident on any port is divided equally between two other ports with a 90° phase difference, and the fourth port is isolated. The waveguide form of quadrature hybrid consists of two parallel waveguides coupled through a series of apertures or branch waveguides. The latter is commonly called a branch-line coupler and is the choice for the present design because of its ease of construction as a split block and the possibility of combining multiple hybrids in a single split block structure as proposed in [2]. In an E-plane branch-line coupler, the branch guides are between the broad walls of the main waveguides so there is a plane of symmetry through the centers of the broad walls of all the waveguides. As no currents flow across this plane of symmetry, a coupler may be split in this plane without concern that imperfect contact between the two halves might affect the performance of the circuit.

The amplitude and phase imbalance at the outputs of a quadrature hybrid affect the LO noise rejection of a balanced mixer and the image rejection of a sideband-separating mixer. Fig. 1 shows contours of constant image rejection (or LO noise rejection) on the amplitude imbalance vs. phase imbalance plane.

The goal of the present work was to develop two waveguide quadrature hybrids, one with amplitude imbalance $\leq$ 1 dB and phase imbalance $\leq$ 1°, and the other with amplitude imbalance $\leq$ 0.5 dB and phase imbalance $\leq$ 1°. These designs should cover as much as possible of the full waveguide band ($f_{max}/f_{min} \approx 1.5$) and should have dimensions suitable for fabrication on a CNC machine, even when scaled as high in frequency as ALMA Band 9 (602-720 GHz).

Analysis and Optimization

A WR-10 waveguide branch-line hybrid with six branches is shown in Fig. 2(a). The lengths of the branch guides and their spacings are approximately quarter of a guide wavelength at the center frequency of operation. The number of branches, the heights and lengths of the branches, and the heights and lengths of the main waveguide sections between the branches, are parameters which can be varied in optimizing the electrical performance. In the present design, the heights of the waveguide sections are restricted, as described in the next section, to facilitate machining hybrids scaled for operation in the higher frequency bands.

Initially, the hybrid was modeled as a number of E-plane T-junctions, interconnected by waveguides as shown in Fig. 2(b), and analyzed using the microwave circuit simulator MMICAD [3]. An equivalent circuit of an E-plane T-junction, given by Marcuvitz [4], is shown in Fig. 2(c). MMICAD allows a fast optimization of the approximate equivalent circuit of the hybrid. This circuit model does not take into account the weak coupling of evanescent modes between adjacent T-junctions, which leads to a small but significant error when the T-junctions are interconnected by short waveguide sections as in the present work.

The finite-difference time-domain (FDTD) EM simulator QuickWave [5] allows an accurate but slower analysis of the hybrid, including the effects of all modes, propagating and evanescent. To verify the accuracy of the QuickWave analysis, the WR-10 hybrid shown in Fig. 2 was fabricated and measured on a vector network analyzer. Figure 3 shows the measured and simulated results. Note that the measured S_{21} and S_{31} have lower amplitudes than predicted by QuickWave; this is because of waveguide loss in the actual hybrid which was not taken into account in the FDTD analysis. However, the amplitude and phase imbalance curves agree well with the measurements, verifying the accuracy of the software. The QuickWave analysis is well converged after 6,000 iterations and takes about 22 minutes on a 933-MHz Pentium III computer when using 4-port excitation.

Figure 4 shows the results (a) from MMICAD and (b) from QuickWave for the six-branch WR-10 hybrid of Fig. 2(a). The amplitude and phase imbalance are shown in Fig. 4(c). It is clear that the circuit model is not accurate enough for the present work.

To optimize the design of the hybrids, the advantages of the accurate but slow EM simulator (QuickWave) can be combined with those of the fast but approximate circuit simulator (MMICAD) with its powerful optimizer through the *space mapping* technique [6,7]. To use space mapping, the circuit model and the physical structure must have the same variables — *e.g.*, waveguide lengths and heights. The relationship between the parameter spaces of the circuit model and the physical structure is then determined. The fast circuit optimizer can then be used to predict the parameters of an optimum physical structure. In the present hybrid design, it takes 2-4 space mapping iterations to reach an acceptable result.

Design

To meet the requirement that the waveguide hybrids be suitable for fabrication by CNC machine when scaled as high in frequency as ALMA Band 9 (602-720 GHz), the height of the main waveguide sections was fixed at the full height (b = a/2), and the height of the branch guides was limited to $B_n \geq 0.12a$. In the 602-720 GHz band with 0.014" x 0.007" waveguide, this corresponds to a branch height $B_n \geq 0.0017"$. The main guides can be machined using an end mill, and the branch guides can be made with a shaving tool.

Figure 5 shows a six-branch hybrid with the independent parameters labeled. Note that it is symmetrical from end to end — it was found that no advantage was gained by allowing an asymmetrical design with six independent branch heights and five independent spacings. The design variables are: the heights of the branches (B_n), the spacing between branches (L_n), and the distance (L_{11}) between the main waveguides. The simulation and design of the hybrids was done in the WR-10 band (75-110 GHz) to enable prototypes to be measured on a vector network analyzer. The limit on branch guide height requires $B_n \geq 0.012"$. The height of the main waveguide sections is fixed at the standard b = 0.050".

The space mapping design procedure is demonstrated in Fig. 6 for a hybrid with amplitude imbalance $\leq$ 0.5 dB and phase imbalance $\leq 1°$. Figure 6(a) shows the optimized MMICAD solution, which we shall refer to as the *MMICAD reference solution,* and the QuickWave result using the same set of dimensions. Figure 6(b) shows the MMICAD solution after it is re-optimized to match the QuickWave solution (also shown for comparison). The dimensions and differences DLTA1 are shown in the table. The dimensions in the QuickWave model were then changed by –DLTA1, giving the results shown in Fig. 6(c), which also shows the MMICAD reference solution for comparison. This is the end of the first space mapping iteration. The second iteration cycle starts by re-optimizing the MMICAD solution to match the last QuickWave solution, and produces a change of dimensions DLTA2. The dimensions of the QuickWave model are then changed by –DLTA2, and so on. The results of the second iteration are shown in Figs. 6(d) and (e). It is seen that good convergence is achieved.

Results

Hybrids with N = 5, 6 and 7 branches were considered initially. It was found that increasing N from 6 to 7 increased the bandwidth by only a small amount but required smaller branch heights (branch height is approximately proportional to 1/N). It was found that with N = 6, the smallest branch guide height was ~ 0.12a, while N = 7 required branches of height 0.11a and had only a marginally greater bandwidth. Consequently, all the hybrids described here have N = 6 branches. As no design was found which maintained an amplitude balance to within 1 dB over the full waveguide band, three designs were produced with overlapping bands — one to cover the lower part of the band, one for the center of the band, and one for the upper end of the band.

Figures 7-9 show the S-parameters and the amplitude and phase imbalance for the three different designs with amplitude imbalance ≤ 1 dB. Figures 10-12 show the performance of the three hybrids designed with amplitude imbalance ≤ 0.5dB. The dimensions are given in the figures. (Note that in some cases the width of the waveguide was changed slightly to increase the bandwidth). The results are summarized in Table I.

Table I: Data for WR-10 Hybrids

Hybrid	Max ampl. Imbalance dB	Max phase Imbalance deg	F_{min} GHz	F_{max} GHz	F_{max}/F_{min}
Fig. 7	1	1	75.0	106.9	1.43
Fig. 8	1	1	77.8	109.1	1.40
Fig. 9	1	1	79.3	110.0	1.39
Fig. 10	0.5	1	73.8	95.0	1.29
Fig. 11	0.5	1	82.6	106.5	1.29
Fig. 12	0.5	1	83.9	110.0	1.31

The designs given here are for the WR-10 band (75-110 GHz), but they can be scaled for use in any other band by determining the scale factor S which gives the best match of $S.F_{max}$ and $S.F_{min}$ to the desired band. Then, all the dimensions given in the appropriate figure (Figs. 7-12) are divided by S. Table II lists the ALMA bands as of the time of writing.

Table II: ALMA Bands
from the Project Book (1/2001)

Band	F_{min} GHz	F_{max} GHz	F_{max}/F_{min}
1	31.3	45.0	1.44
2	67	90.0	1.34
3	89*	116.0	1.30
<< 3	84*	116.0	1.38 >>
4	125	163.0	1.30
5	163	211.0	1.29
6	211	275.0	1.30
7	275	370.0	1.35
8	385	500.0	1.30
9	602	720.0	1.20
10	787	950.0	1.21

* change to 84 GHz has been proposed

References

[1] E. Bryerton, private communication, Dec. 2000.

[2] S. M. X. Claude, C. T. Cunningham, A. R. Kerr and S. K. Pan, “Design of a Sideband-Separating Balanced SIS Mixer Based on Waveguide Hybrids,” ALMA Memo 316, Sept. 20, 2000.

[3] MMICAD microwave circuit analysis and optimization program, Optotek, Ltd., Ontario, Canada.

[4] N. Marcuvitz, *Waveguide Handbook*, New York: McGraw Hill, 1951. See Chapter 6, p. 236 ff.

[5] QuickWave EM simulator, QWED s.c., Zwyciezcow 34/2, 03-938 Warsaw, Poland.

[6] J. W. Bandler, R. M. Biernacki, S. H. Chen, R. H. Hemmers and K. Madsen, “Aggressive Space Mapping for Electromagnetic Design,” *IEEE MTT-S Int. Microwave Symp. Dig.*, June 1995, pp. 1455-1458.

[7] J. W. Bandler, R. M. Biernacki, S. H. Chen and Y. F. Huang, “Design Optimization of Interdigital Filters Using Aggressive Space Mapping and Decomposition,” *IEEE Trans. Microwave Theory Tech.*, vol. MTT-45, pp. 761-769, May 1997.

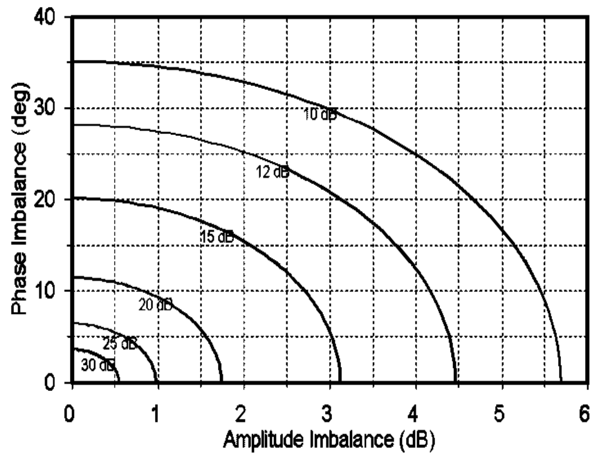

Fig. 1. Contours of constant image rejection (or LO noise rejection) on the amplitude imbalance vs. phase imbalance plane.

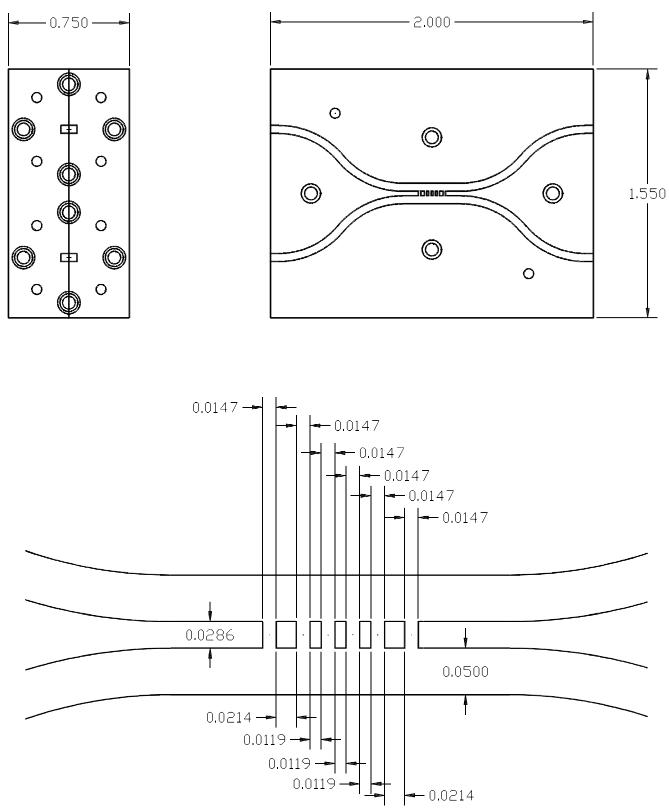

Fig. 2(a). WR-10 waveguide quadrature hybrid with six branch lines (dimensions in inches).

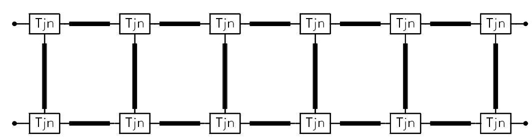

Fig. 2(b). A six-branch hybrid represented as twelve interconnected T-junctions.

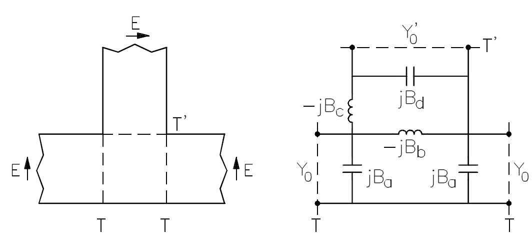

Fig. 2(c). Approximate equivalent circuit of an E-plane T-junction (from [4]). Dashed lines indicate the reference planes. Expressions for the element values are given in [4].

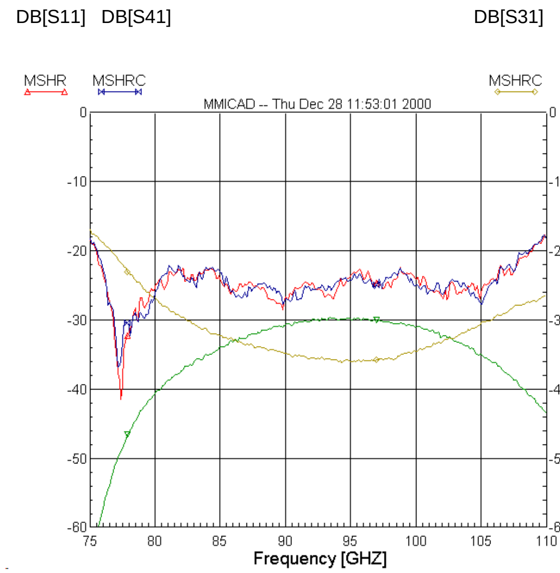

(a)

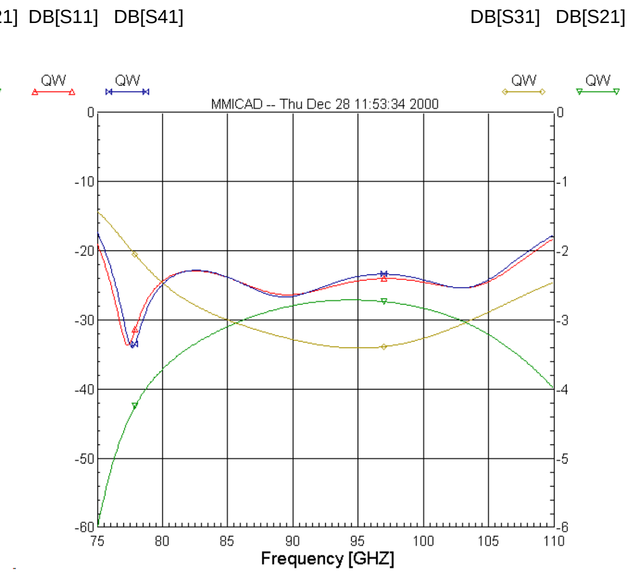

(b)

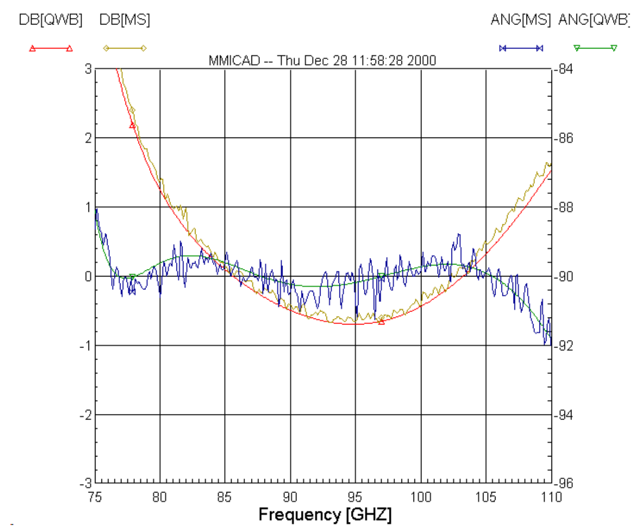

(c) Measured [MS] & QuickWave [QWB]

Fig. 3. Comparison of results for the six branch WR-10 hybrid of Fig. 2: (a) Measurements with the vector network analyzer. (b) Results obtained using the FDTD EM simulator (QuickWave). (c) Amplitude and phase imbalance — from the measured (noisy) and simulated (smooth) results.

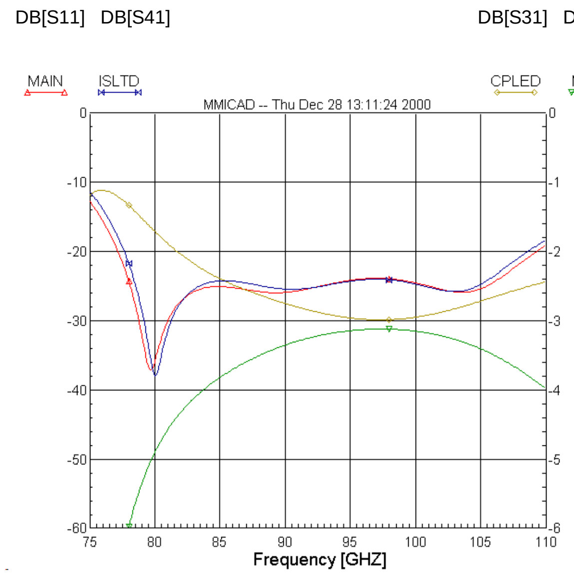

(a) MMICAD

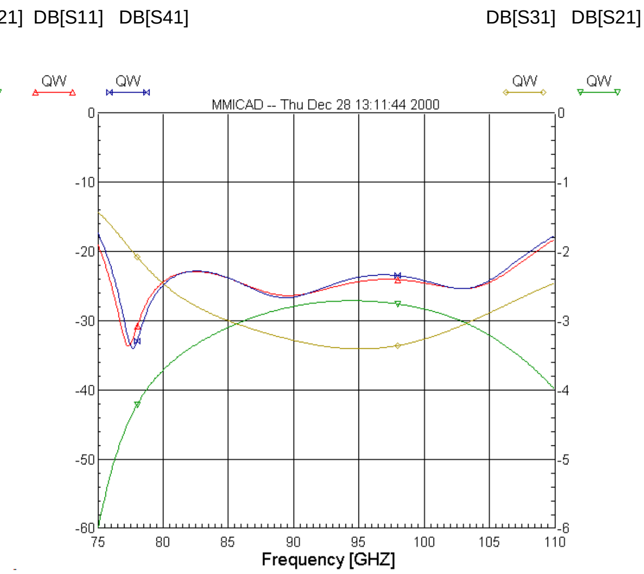

(b) QuickWave FDTD

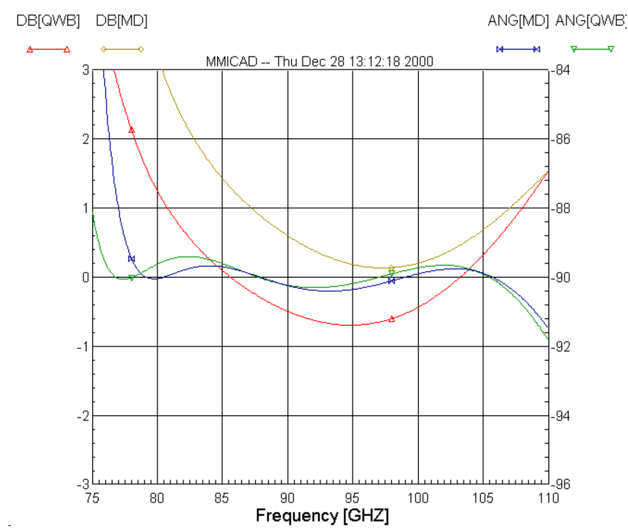

(c) MMICAD [MD] & QuickWave [QWB]

Fig. 4. Comparison of results for the six-branch WR-10 hybrid of Fig. 2: (a) From the circuit model using MMICAD. (b) From the FDTD EM simulation using QuickWave. (c) Amplitude and phase imbalance. It is clear that the circuit model (MMICAD) alone is not accurate enough for the present work.

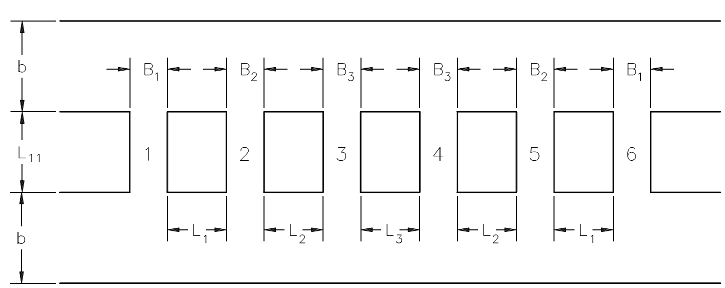

Fig. 5. A six-branch hybrid ($N = 6$) showing the design variables: the heights of the branch waveguides (B_n), the spacing between branches (L_n), and the length (L_{11}) of the branches.

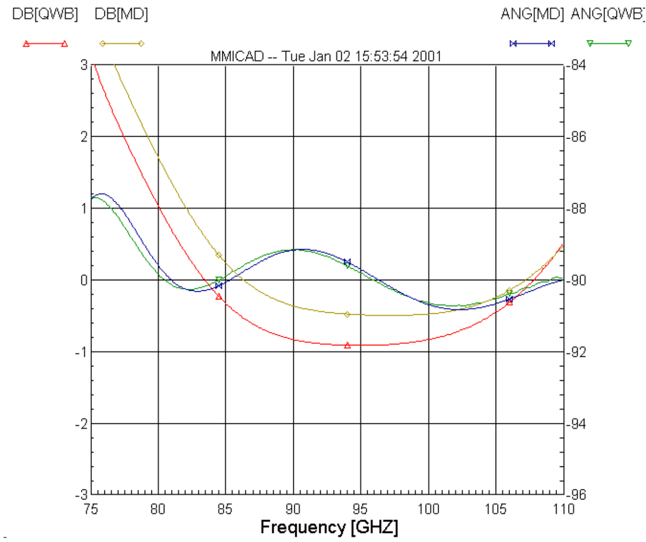

	MD1	QW1		MD1	QW1
B_1	0.01320	0.01320	L_1	0.02550	0.02550
B_2	0.01260	0.01260	L_2	0.02730	0.02730
B_3	0.01580	0.01580	L_3	0.02590	0.02590
			L_{11}	0.02800	0.02800

Fig. 6(a). MD1 & QW1.

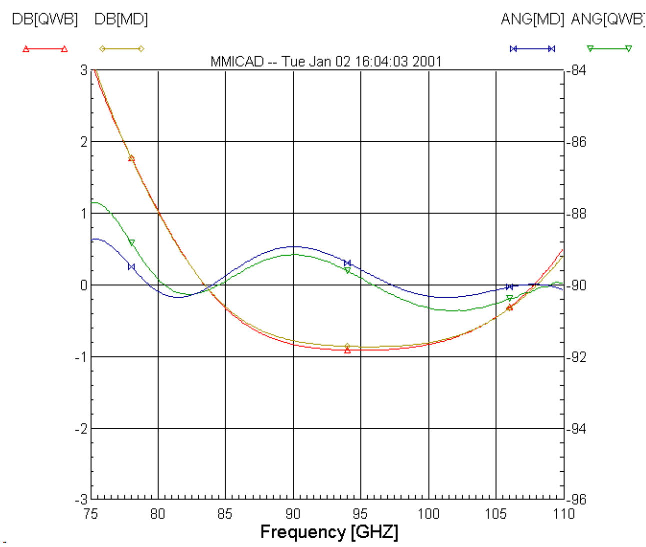

	MD1	MD2	DLTA1		MD1	MD2	DLTA1
B_1	0.01320	0.01276	0.00044	L_1	0.02550	0.02795	-0.00245
B_2	0.01260	0.01240	0.00020	L_2	0.02730	0.02890	-0.00160
B_3	0.01580	0.01530	0.00050	L_3	0.02590	0.02176	0.00414
				L_{11}	0.02800	0.02858	-0.00058

Fig. 6(b). MD2 & QW1.

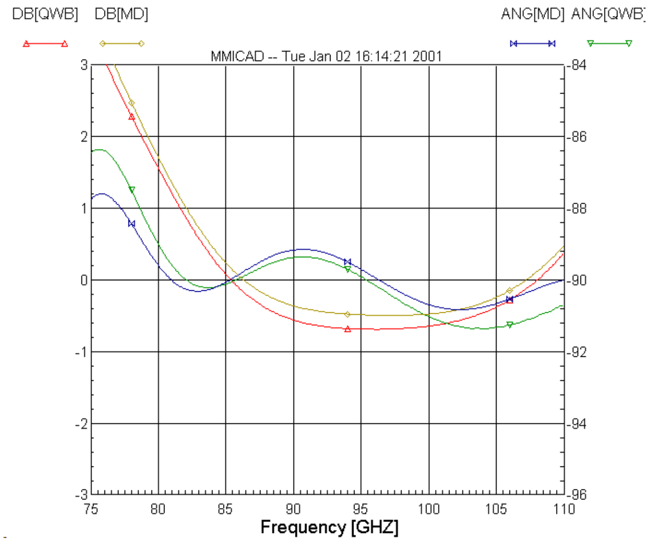

	QW1	DLTA1	QW2		QW1	DLTA1	QW2
B_1	0.01320	0.00044	0.01364	L_1	0.02550	-0.00245	0.02305
B_2	0.01260	0.00020	0.01280	L_2	0.02730	-0.00160	0.02570
B_3	0.01580	0.00050	0.01630	L_3	0.02590	0.00414	0.03004
				L_{11}	0.02800	-0.00058	0.02742

Fig. 6(c). MD1 & QW2.

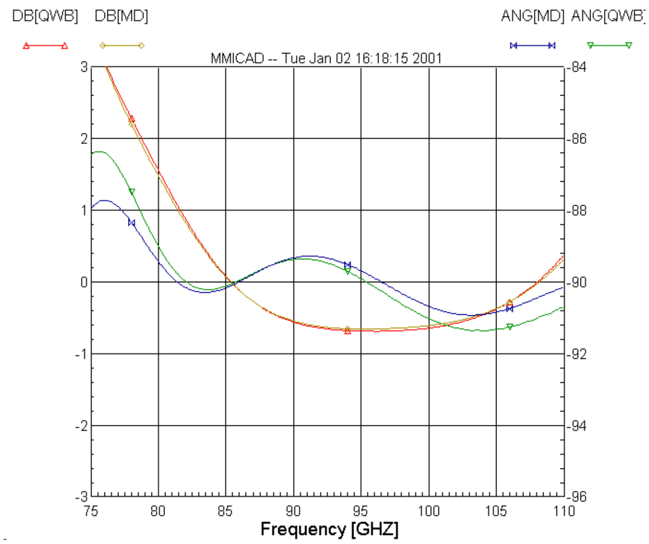

	MD1	MD3	DLTA2		MD1	MD3	DLTA2
B_1	0.01320	0.01303	0.00017	L_1	0.02550	0.02534	0.00016
B_2	0.01260	0.01243	0.00017	L_2	0.02730	0.02651	0.00079
B_3	0.01580	0.01557	0.00023	L_3	0.02590	0.02603	-0.00013
				L_{11}	0.02800	0.02828	-0.00028

Fig. 6(d). MD3 & QW2.

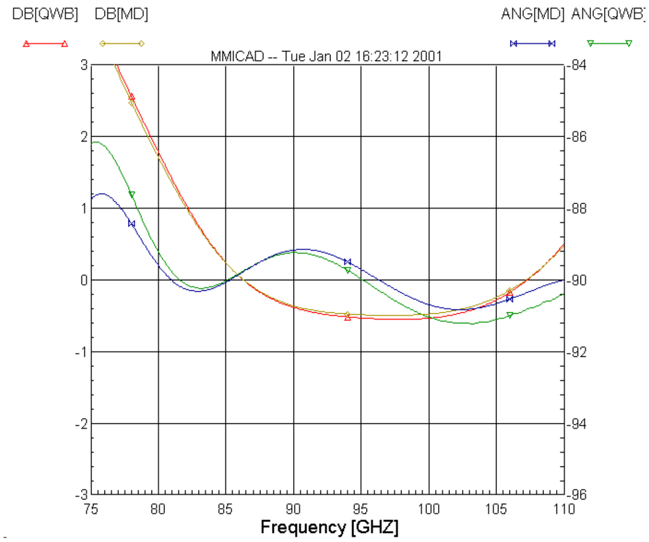

	QW2	DLTA2	QW3		QW2	DLTA2	QW3
B_1	0.01364	0.00017	0.01381	L_1	0.02305	0.00016	0.02321
B_2	0.01280	0.00017	0.01297	L_2	0.02570	0.00079	0.02649
B_3	0.01630	0.00023	0.01653	L_3	0.03004	-0.00013	0.02991
				L_{11}	0.02742	-0.00028	0.02714

Fig. 6(e). MD1 & QW3.

Fig. 6. The space mapping procedure, demonstrated for a six-branch hybrid with amplitude imbalance $\leq$ 0.5 dB and phase imbalance $\leq 1^\circ$. (a) The optimized MMICAD solution: the MMICAD reference solution (MD1), and the QuickWave result (QW1) using the same set of dimensions. (b) The MMICAD solution after it is re-optimized (MD2) to match the QuickWave solution (also shown for comparison) resulting in change of dimensions DLTA1. The dimensions in the QuickWave model were then changed by –DLTA1, giving the results (QW2) shown in (c), with the MMICAD reference solution (MD1) for comparison. That ends the first space mapping iteration. The second iteration starts by re-optimizing the MMICAD solution (MD3) to match the last QuickWave solution (QW2) to produce a change of dimensions DLTA2 relative to the MMICAD reference solution. The dimensions of the QuickWave model are then changed by –DLTA2, and so on. The results of the second iteration are shown in Figs. 6(d) and (e).

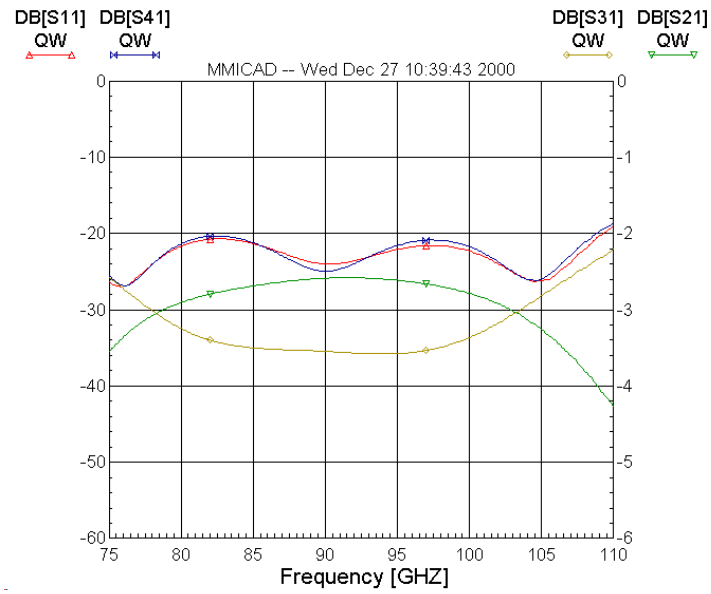

(a)

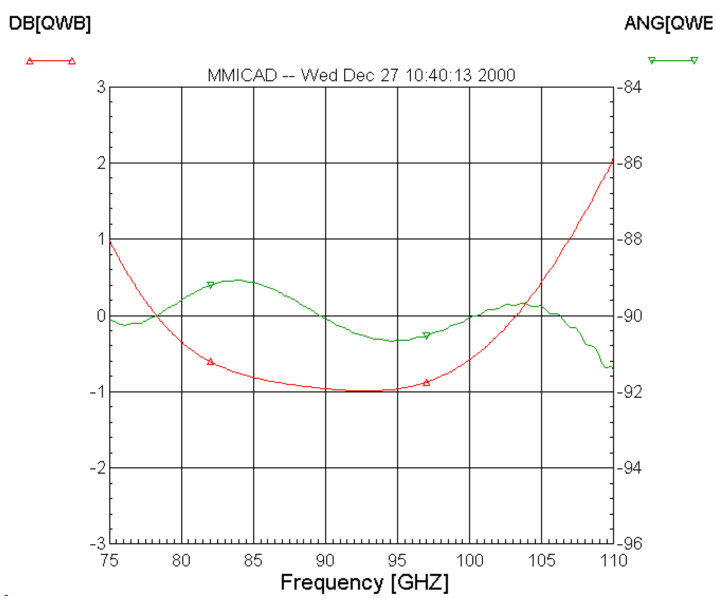

(b)

a = 0.1100	B_1 = 0.0134	L_1 = 0.0300	L_{11} = 0.0288
b = 0.0500	B_2 = 0.0124	L_2 = 0.0280	
	B_3 = 0.0153	L_3 = 0.0256	

Fig. 7. QuickWave results for a hybrid with amplitude imbalance ≤ 1 dB and phase imbalance ≤ 1° over 75.0-106.9 GHz (1.43:1). (a) S-parameters. (b) Amplitude and phase imbalance.

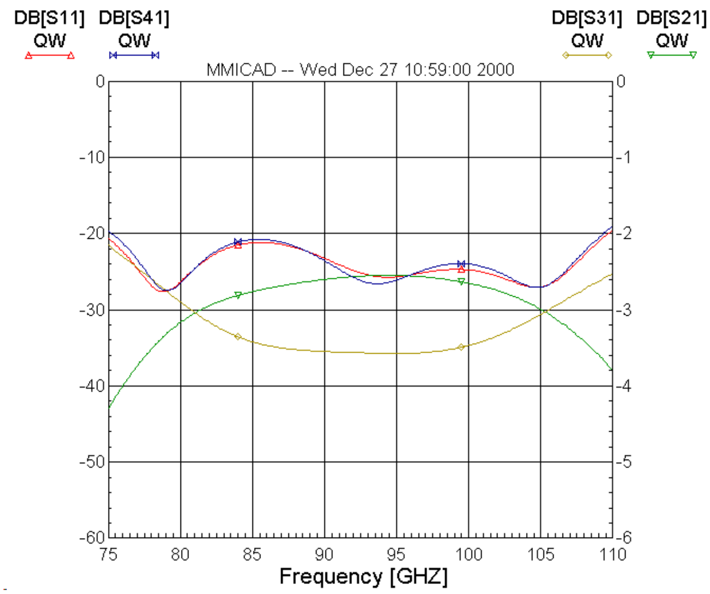

(a)

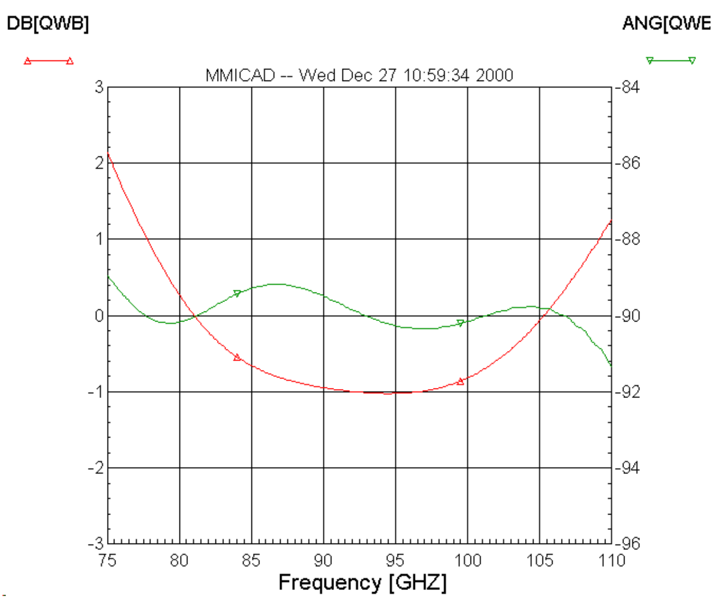

(b)

a = 0.1030	B_1 = 0.0129	L_1 = 0.0300	L_{11} = 0.0286
b = 0.0500	B_2 = 0.0132	L_2 = 0.0280	
	B_3 = 0.0150	L_3 = 0.0236	

Fig. 8. QuickWave results for a hybrid with amplitude imbalance $\leq$ 1 dB and phase imbalance $\leq$ 1° over 77.8-109.1 GHz (1.40:1). (a) S-parameters. (b) Amplitude and phase imbalance.

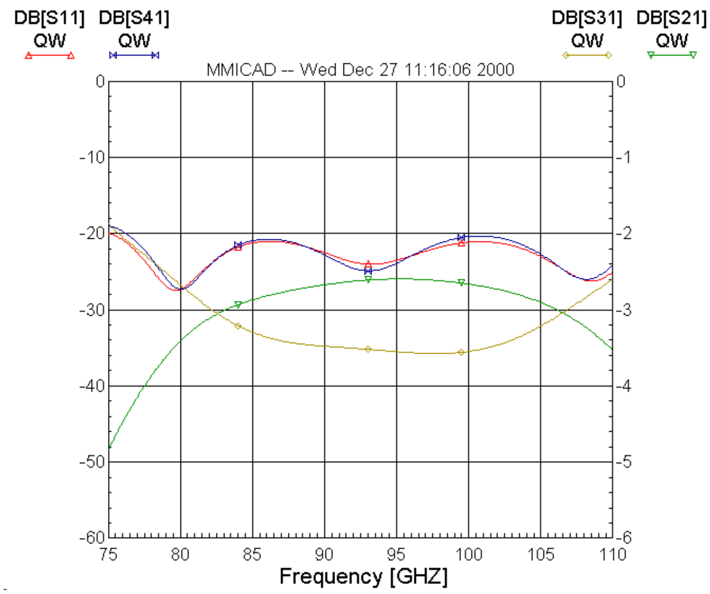

(a)

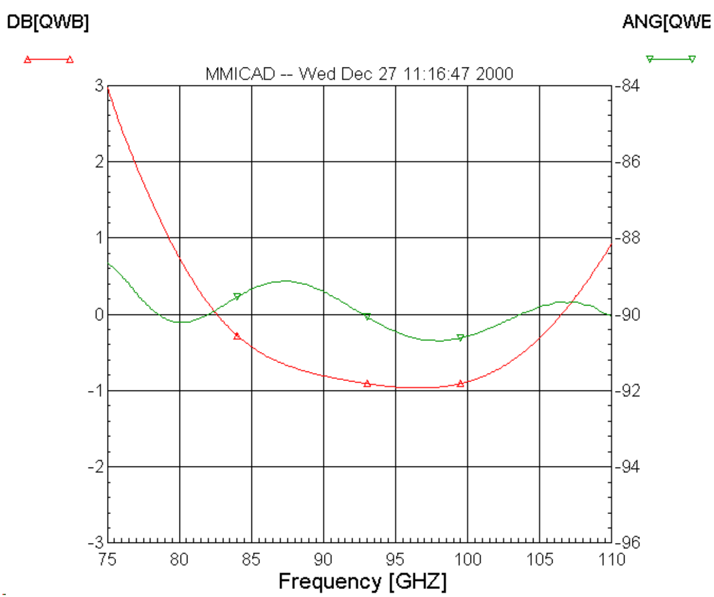

(b)

a = 0.1000	B_1 = 0.0131	L_1 = 0.0302	L_{11} = 0.0285
b = 0.0500	B_2 = 0.0123	L_2 = 0.0273	
	B_3 = 0.0159	L_3 = 0.0257	

Fig. 9. QuickWave results for a hybrid with amplitude imbalance $\leq$ 1 dB and phase imbalance $\leq$ 1° over 79.3-110.0 GHz (1.39:1). (a) S-parameters. (b) Amplitude and phase imbalance.

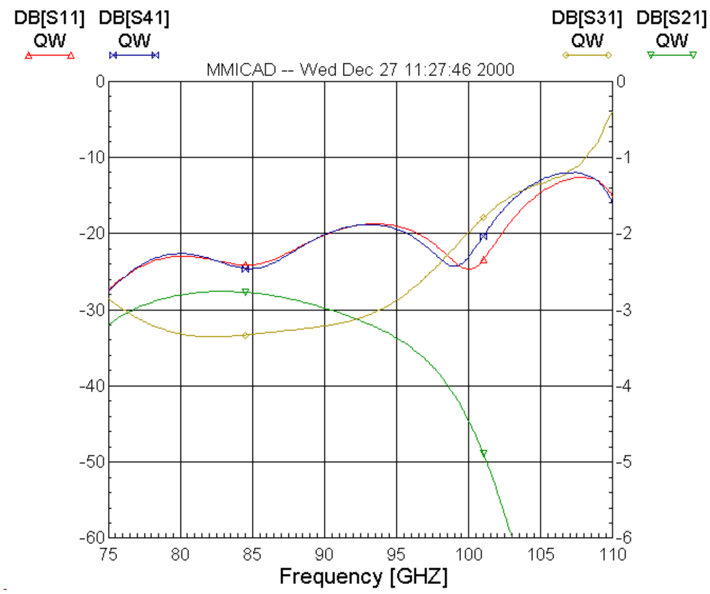

(a)

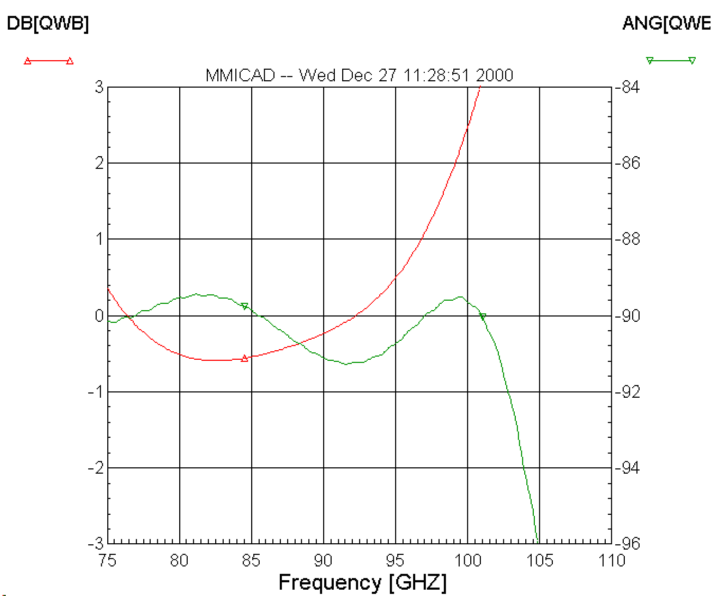

(b)

a = 0.1050	B_1 = 0.0120	L_1 = 0.0377	L_{11} = 0.0362
b = 0.0500	B_2 = 0.0128	L_2 = 0.0255	
	B_3 = 0.0161	L_3= 0.0238	

Fig. 10. QuickWave results for a hybrid with amplitude imbalance $\leq$ 0.5 dB and phase imbalance $\leq 1^\circ$ over 73.8-95.0 GHz(1.29:1). (a) S-parameters. (b) Amplitude and phase imbalance.

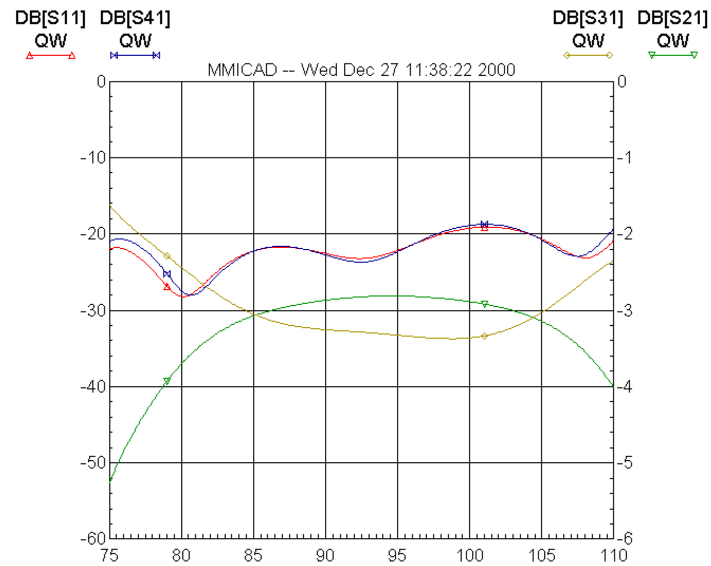

(a)

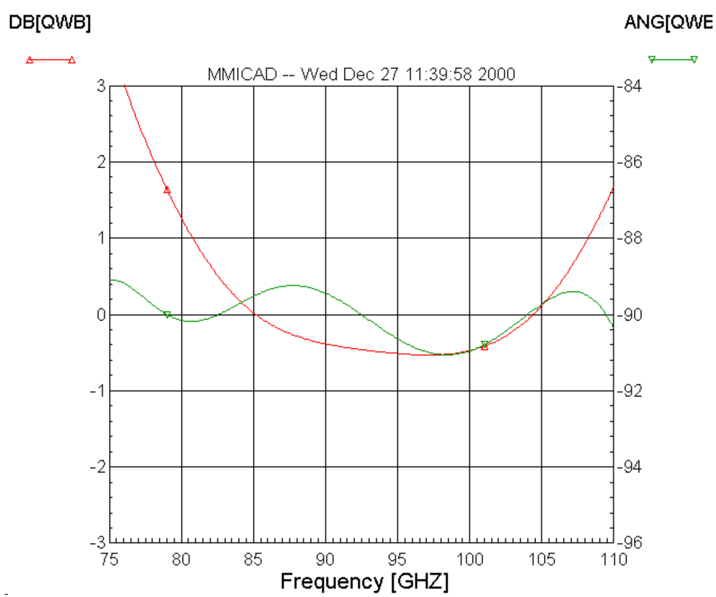

(b)

a = 0.1000	B_1 = 0.0142	L_1 = 0.0325	L_{11} = 0.0285
b = 0.0500	B_2 = 0.0141	L_2 = 0.0229	
	B_3 = 0.0147	L_3 = 0.0207	

Fig. 11. QuickWave results for a hybrid with ampl. imbalance $\leq$ 0.5 dB and phase imbalance $\leq$ 1° over 82.6-106.5 GHz (1.29:1). (a) S-parameters. (b) Amplitude and phase imbalance.

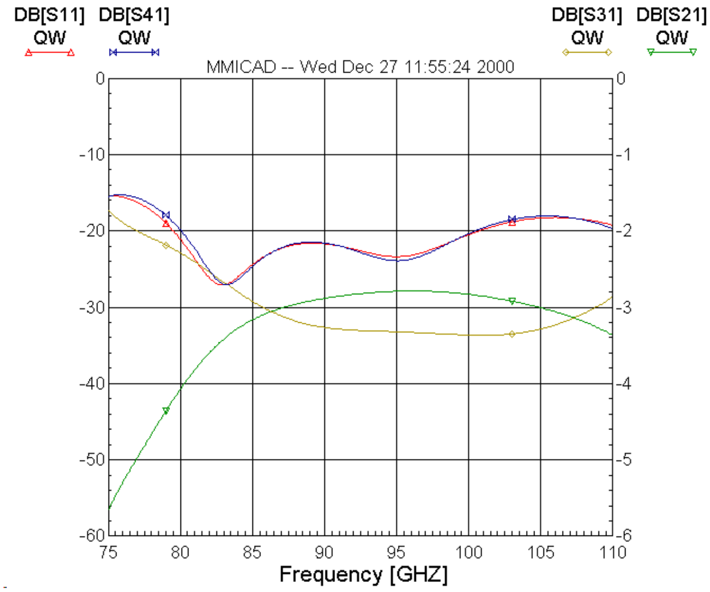

(a)

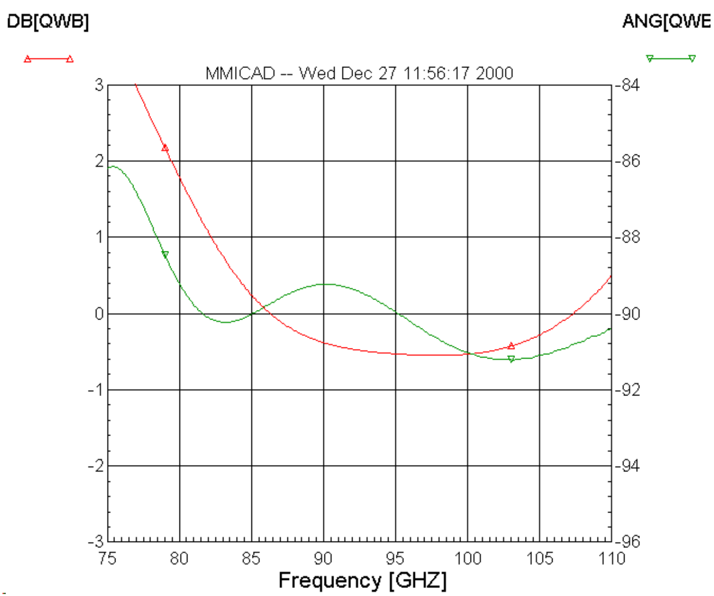

(b)

a = 0.1000	B_1 = 0.0138	L_1 = 0.0232	L_{11} = 0.0271
b = 0.0500	B_2 = 0.0130	L_2 = 0.0265	
	B_3 = 0.0165	L_3 = 0.0299	

Fig. 12. QuickWave results for a hybrid with ampl. imbalance $\leq$ 0.5 dB and phase imbalance $\leq 1^\circ$ over 83.9-110.0 GHz (1.31:1). (a) S-parameters. (b) Amplitude and phase imbalance.